JOURNAL OF MATERIALS SCIENCE 21 (1986) 3183–3193

Tensile microstrain properties of vapour quenched and rolled Al-alloys

P. G. PARTRIDGE
Materials and Structures Department, Royal Aircraft Establishment, Farnborough, Hants, UK
W. BONFIELD
Department of Materials, Queen Mary College, London E1 4NS, UK

Al-alloy deposits produced by quenching from the vapour phase were rolled into sheet and tensile stress–strain curves were obtained in the microstrain region ($<10^{-4}$ strain). Two binary alloys (Al–5% Cr and Al–11% Cr) and two ternary alloys (Al–8% Cr–1.2% Fe and Al–6% Cr–1.0% Fe) were tested (compositions in wt%). The corresponding tensile strengths were 375 and 590 MPa for the binary alloys, and 679 and 662 MPa for the ternary alloys. The microyield stresses (the stress to produce a residual plastic strain of 2×10^{-6}) for the vapour quenched alloys were less than 26 MPa compared with 100 to 260 MPa for commercial aluminium alloys. When the vapour quenched alloys were retested immediately after prestrain, the values were much greater (166 to 254 MPa), but after resting at room temperature for 7 to 106 days low values were again obtained. The low microyield stresses were attributed to the high density of dislocations present in the rolled sheet and the behaviour observed may be characteristic of high strength dispersion hardened Al-alloys produced by rapid solidification and rolling.

1. Introduction

Al-alloys have been produced by electron beam evaporation and vapour deposition onto cooled substrates [1, 2]. These alloys contained a supersaturated and metastable solid solution in which was embedded a high volume fraction of dispersed phase [2]. This microstructure led to high strength and Young's modulus values at room and elevated temperature, with large proof ultimate ratios.

One possible application for such alloys is in gyroscopes [3, 4]. Dimensional stability and completely elastic behaviour with minimum hysteresis are required under the very low loads encountered in service and these properties must be retained after repeated temperature and load cycles.

The selection of the best material for use in gyroscopes cannot be based upon the tensile data obtained in conventional engineering tests [4, 5]. Tests have therefore been developed which enable the tensile stress–strain curve to be measured in the microstrain region, i.e. at strains less than 10^{-4}.

This paper describes the stress–strain curves obtained in the microstrain region for vapour quenched and rolled alloys. The curves are compared with those obtained for conventional Al-alloys and discussed in terms of the strain hardening mechanisms in dispersion hardened alloys.

2. Experimental technique

The evaporation and vapour quenching techniques have been described elsewhere [1, 2]. The alloy vapour was condensed onto water cooled substrates until the deposit thickness was about 30 mm (Fig. 1). These deposits were pressed and rolled into a 1.6 mm sheet. Alloy compositions, substrate temperatures and working conditions are given in Table I. Nearly all the chromium was in solid solution in the Al–5% Cr alloy, but some $CrAl_7$ particles about 0.1 μm diameter were present in grain boundaries. In the more highly alloyed Al–11% Cr alloy most of the chromium was again in solid solution, but a fine dispersion of chromium-rich particles 3 nm in diameter was present within the grains. Most of the chromium was also in solid solution in the ternary Al–Cr–Fe alloys, but in these alloys a uniform dispersion of 3 nm diameter iron–chromium particles was obtained (Fig. 2). The grains were pancake shaped and typically 1 to 4 μm in diameter in the sheet plane and 0.1 μm thick.

Tensile test pieces had a 30 mm parallel portion and minimum radii between the gauge length and test piece head. Measurements of the microscopic yield stress (the stress to cause a residual plastic strain of 2×10^{-6}) were made [6] with a Tuckerman optical strain gauge of sensitivity 2×10^{-6}. After equilibration for 30 min at room temperature, the zero point was measured and the specimen was then strained at a constant rate of $3.3 \times 10^{-4}\,sec^{-1}$ to a given load. This load was held constant for 30 sec in order to observe the total extension; the specimen was then unloaded at a strain rate equal to the loading rate and the zero point was measured again. This procedure was repeated for a series of increasing tensile loads, the zero point and total extension being measured at each load. The microscopic yield point was determined by a shift in zero reading, which gave a direct measure of plastic strain.

The tests were carried out on as-rolled material and on annealed material. The loading sequence used for each test piece is summarized in Table II. The stress–

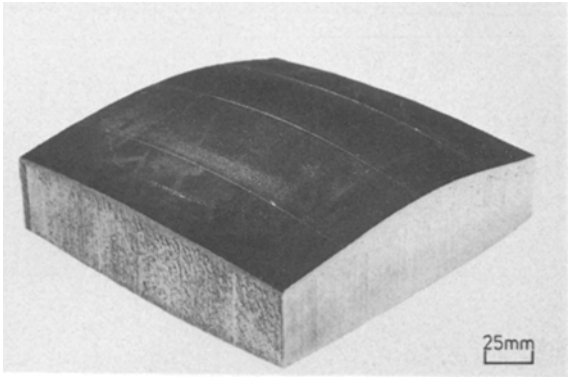

Figure 1 Deposit after removing from collector and edge trimming.

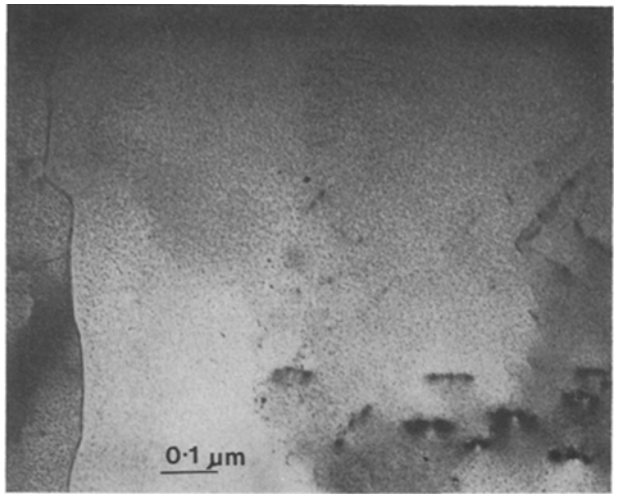

Figure 2 Transmission electron micrograph showing fine precipitates in Al–Cr–Fe alloy.

strain curves were determined for as-rolled material up to a plastic strain of about 10^{-3} (Curve 1 in Table II). Some tests were then repeated to check whether the stress–strain curve depended on prestrain (Curve 2). A second repeat was then carried out after the test piece had rested one week at room temperature (Curve 3). The numbering of the curves is used to identify the stress–strain history in subsequent figures. Tests on annealed material followed a similar sequence (Table II). Three of the test pieces were tested after annealing first at 325° C for 2 h (Curves 1 and 2 in Table II) and then at 500° C for 65 h (Curves 3–6 in Table II).

The binary Al–12% Cr alloy test piece and the ternary Al–8% Cr–1.2% Fe alloy test piece were finally pulled to fracture and the tensile properties determined.

Tests were also carried out on commercial purity aluminium and L70 aluminium alloy. The commercial purity alloy contained 0.5% Fe and 0.2% Si and was tested in the as-received cold rolled condition, and in the annealed condition after 1 h at 250° C. The L70 alloy contained 4% Cu, 0.8% Si, 0.8% Mg, 0.7% Mn, and 0.5% Fe and was solution treated and cold worked. The L70, alloy naturally aged at room temperature, has a tensile strength of about 400 MPa and is equivalent to 2014-T3 alloy. The results were compared with those obtained for vapour quenched alloys.

3. Results

3.1. Stress–strain curves of as-rolled and prestrained material

The stress–strain curves are shown in Fig. 3. All the test pieces in the as-rolled state (Curve 1) showed significant plastic microstrain at very low stresses and the microyield stresses did not exceed 26 MPa (Table III). With the exception of the Al–12% Cr alloy, all the alloys showed three stages in the stress–strain curves. In the initial Stage 1 a plastic strain between 6×10^{-6} and 51×10^{-6} was obtained under conditions of low strain hardening rate (SHR). This was followed by a Stage 2 in which the SHR was very high and a Stage 2 in which the SHR fell to a low value (Fig. 4). The beginning of Stage 3 corresponds to the onset of macroscopic yielding; the yield stress σ_{ys} [taken to be the stress at the end of Stage 2 beyond which the SHR $d\sigma/d\varepsilon$ was less than 2.5×10^6 MPa (Fig. 4)] is reached at the limit of proportionality in a conventional tensile test. Values of σ_{ys} obtained for as-rolled material in the present tests were between 280 and 450 MPa (Table III). Stage 1 was not observed in the test on the Al–12% Cr alloy test piece (Fig. 3b).

The limits of Stages 1 and 2, as defined by the co-ordinates $(\sigma_1, \varepsilon_1)$ and $(\sigma_{ys}, \varepsilon_1)$, respectively, in Fig. 4 are tabulated in Table IV. The increase in flow stress $\Delta\sigma$ in Stage 2 (Fig. 4) was between 225 and 296 MPa (Table IV).

In the curves obtained after prestrain (Curve 2 in Fig. 3a, b and d) Stage 1 was absent and the values of the microyield stresses (166 to 254 MPa) and the macroyield stresses (400 to 562 MPa) were greater than before prestrain (Table III) and the $\Delta\sigma$ values were between 146 and 336 MPa (Table IV).

The curves obtained after the test pieces had been held at room temperature for one week, showed that

TABLE I Alloy data and working operations

Alloy (wt %)	Substrate temperature (° C)	Working operations			
		Pressing		Rolling	
		Temperature (° C)	Reduction (%)	Temperature (° C)	Reduction (%)
Binary					
Al–5% Cr	334–372	270	49	255	72
Al–12% Cr	250–277	290	16	280	51
Ternary					
Al–8% Cr–1.2% Fe	244–255	284	40	265	76
Al–6% Cr–1.0% Fe	246–255	270	36	270	79

TABLE II Summary of tensile test programme on vapour quenched alloys

Alloy (wt %)	Tests on as-rolled and prestrained material Test sequence 1–3			Tests on material prestrained in tests 1–3 and annealed at 325° C and 500° C Test sequence 1–6					
	1.* As-rolled	2. Immediate retest after (1)	3. Retested one week after (2)	1. Annealed for 2 h at 325° C	2. Immediate retest after (1)	3. Annealed for 65 h at 500° C after (2)	4. Immediate retest after (3)	5. Retested 106 days after (4)	6. Immediate retest after (5)
Binary									
Al–5% Cr	x	x	x	x	x				
Al–12% Cr	x	x		x	x	x	x	x	x
Ternary									
Al–8% Cr–1.2% Fe	x		x	x	x	x	x	x	x
Al–6% Cr–1.0% Fe	x	x	x†						

*Numbers refer to curves in Figs 3 and 6.
† Test piece cracked after test.

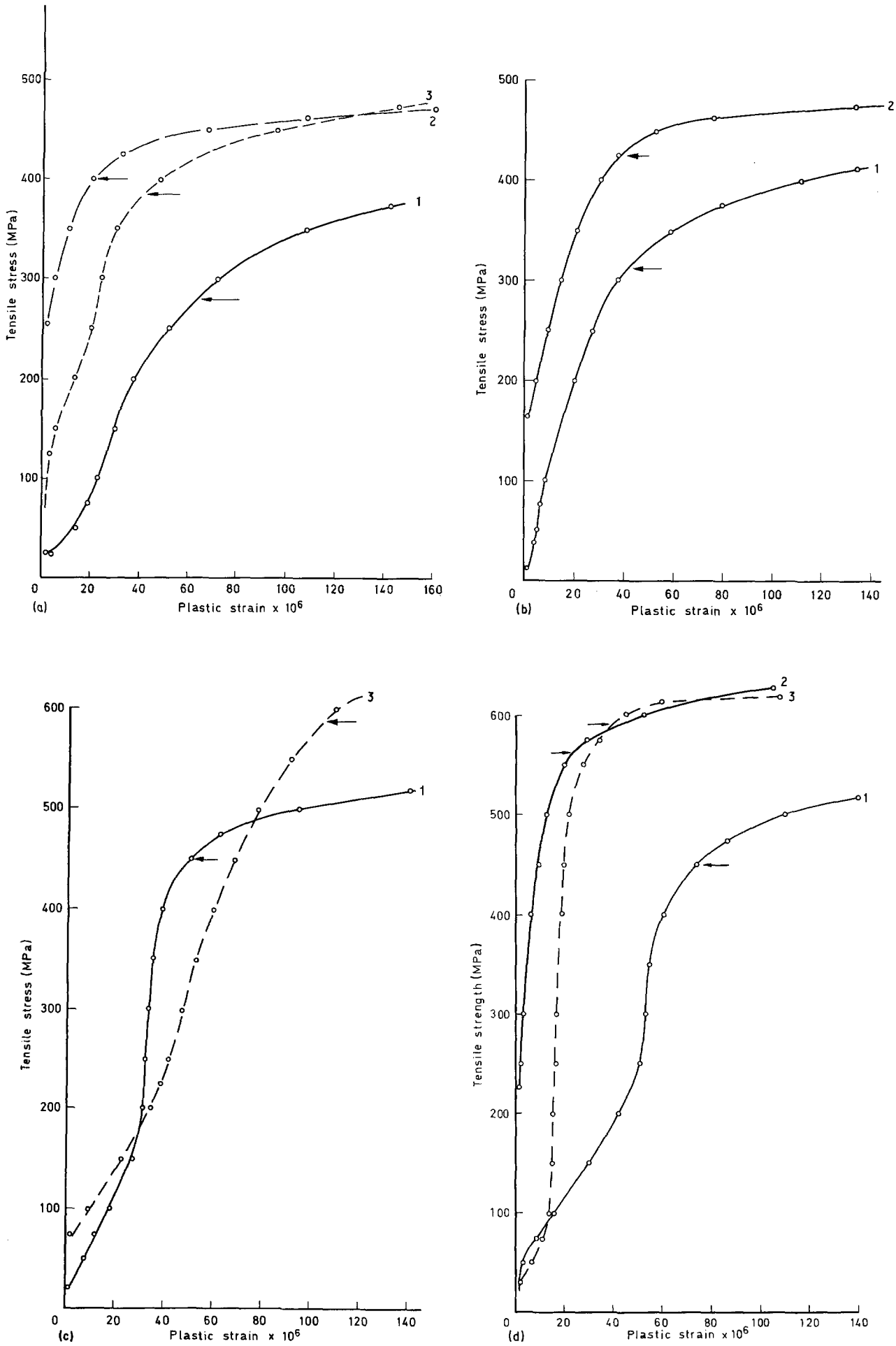

Figure 3 Tensile–microstrain curves. (a) Al–5% Cr alloy, (b) Al–12% Cr alloy, (c) Al–8% Cr–1.2% Fe alloy, (d) Al–6% Cr–1.0% Fe alloy. Test sequence 1–3; 1, as-rolled; 2, retested immediately after (1); 3, after seven days at room temperature. →, σ_{ys}.

TABLE III Microyield and macroyield stresses of vapour quenched and commercial Al-alloys

Alloy (wt %)	Microyield stress and macroyield stress (MPa)					
	1. As-rolled material		2. Immediate retest after prestrain in (1)		3. Retested 1 week after (2)	
	Microyield stress	Macroyield stress σ_{ys}	Microyield stress	Macroyield stress σ_{ys}	Microyield stress	Macroyield stress σ_{ys}
Binary						
Al–5% Cr	26	280	254	400	70	385
Al–12% Cr	16	312	166	425		
Ternary						
Al–8% Cr–1.2% Fe	21	450			70	588
Al–6% Cr–1.0% Fe	22	450	226	562	26	590
Commercial Al-alloy						
pure Al						
As-received	35	100				
After 1 h at 250° C	22	64				
L70 as-received	105	245	190	–	190	
2014–T6	262*					
2024–T4	199–245*					
6061–T6	187–174*					
5456–H34	134–149*					

*Stress to give 1×10^{-6} strain. The approximate tensile strengths of these alloys are 490 MPa (2014–T6), 450 MPa (2024–T4), 250 MPa (6061–T6) and 310 MPa (5456–H34).

Stage 1 was again present (Curve 3, Fig. 3a, c and d) and that the microyield stresses (26 to 70 MPa) were less than after prestrain (Table III); however there was little change in the macroyield stress σ_{ys} (Table III).

Data for commercial aluminium alloys are included in Tables III and IV. Stage 1 was absent in the test on the commercial L70 alloy [7] and was not observed in other tests on commercial aluminium alloys [5]. The microyield stress of commercial purity aluminium (22 to 35 MPa) was similar to that of the vapour quenched alloys in the as-rolled state (Table III).

Compared with the conventional Al alloys, the microyield stresses for vapour quenched alloys were much smaller (especially relative to the L70 alloy σ_{ys} value) and were more strain and time dependent as shown in Fig. 5a. The σ_{ys} values for the vapour quenched alloys were strain dependent but less time dependent than the microyield stress (Fig. 5b).

The maximum σ_{ys} values after prestrain (Curves 2 and 3 in Table III) lay between the limit of proportionality and the 0.1% proof stress measured for the Al–12% Cr alloy and the Al–Cr–Fe alloys using test pieces cut from the same sheet (Table V), but corresponded to the ultimate tensile strength of the Al–5% Cr alloy (Table V).

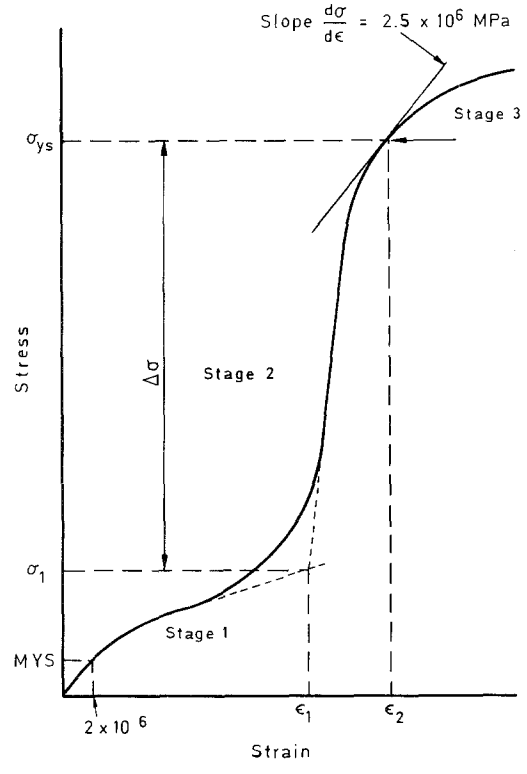

Figure 4 Schematic diagram of Stages 1–3 in microstrain curve.

3.2. Stress–strain curves of annealed and prestrained material

After annealing for 2 h at 325° C (Table VI) the microyield stresses were similar to those obtained in the as-rolled state and less than those obtained after resting for one week at room temperature (Table III).

A comparison of the maximum σ_{ys} values obtained after prestrain (Curves 2 and 3, Table III) with values after annealing at 325° C (Curve 1 in Table VI) shows that annealing reduced σ_{ys} by 10 to 29% in the Al–Cr alloys but had a negligible effect on the more stable ternary Al–Cr–Fe alloy. No change in microstructure was detected after this anneal.

The stress–strain curves for the Al–5% Cr and Al–8% Cr–1.2% Fe alloys (Figs 6a and c) had three stages, but the curve for Al–12% Cr alloy (Fig. 6b) had no Stage 1, which was similar to the behaviour found for these test pieces in the as-rolled state (Fig. 3). However an exceptionally large strain of 10^{-4} was obtained in Stage 1 for the Al–8% Cr–1.2% Fe alloy (Fig. 6c). This suggests that annealing increased the dislocation mobility in Stage 1.

When the test pieces were retested after prestrain (Curves 2 in Fig. 6) Stage 1 was absent and the microyield stresses were very much greater than after annealing (Table VI) and about the same as for prestrained

TABLE IV The plastic strains and stresses at the beginning and end of Stage 2 of the stress–strain curves of vapour quenched Al-alloys and commercial Al-alloys

Alloy (wt %)	Initial loading of test piece					Immediate reloading after prestrain of $\sim 10^{-3}$				
	Beginning of stage 2*		End of stage 2*		$\Delta\sigma = \sigma_{ys} - \sigma_1$	Beginning of stage 2*		End of stage 2*		$\Delta\sigma = \sigma_{ys} - \sigma_1$
	$\varepsilon_1 \times 10^6$	σ_1 (MPa)	$\varepsilon_2 \times 10^6$	σ_{ys} (MPa)	(MPa)	$\varepsilon_1 \times 10^6$	σ_1 (MPa)	$\varepsilon_2 \times 10^6$	σ_{ys} (MPa)	(MPa)
Vapour quenched alloys										
Binary										
Al–5% Cr	6	30	64	280	250	2†	254	20	400	146
Al–12% Cr	2†	16	42	312	296	2†	166	40	425	259
Ternary										
Al–8% Cr–1.2% Fe	30	162	50	450	288		226			
Al–6% Cr–1.0% Fe	47	225	73	450	225	2†		23	562	336
Commercial alloys										
Commercial purity aluminium	2	35	15	100	65	2	105			
L70	2	105	5	245	140	2	190			

*See Fig. 4.
†When $\varepsilon_1 = 2 \times 10^{-6}$, σ_1 corresponds to the microyield stress.

TABLE V Engineering tensile properties

Tensile properties	Vapour quenched aluminium alloys						Commercial aluminium alloys	
	Binary alloys			Ternary alloys			Commercial purity aluminium as-received	L70
	Al–5% Cr	Al–12% Cr		Al–8% Cr–1.2% Fe		Al–6% Cr–1.0% Fe		
	As-rolled	As-rolled	After all microstrain tests*	As-rolled	After all microstrain tests*	As-rolled		
Tensile strength (MPa)	375	590	362	679	365	662	135	400
0.5% proof stress (MPa)	375	585	339	675	336	655		
0.2% proof stress (MPa)	366	564	309	655	295	628		260
0.1% proof stress (MPa)	349	539	284	630	268	598		
Limit of proportionality (MPa)	–	376	113	252	93	449		
Young's modulus (GPa)	77	90	100	88	88	81	69	74
Uniform elongation (%)	–	1.4	1.4	1.0	1.2	0.6		
Total elongation (%)	14	10.4	2.2	9.8	1.8	7.6		13
Hardness HV5	144	185–210		214–219			194	

*The tests are given in Tables II, III and V.

TABLE VI The microyield and macroyield stresses for vapour quenched Al-alloys after annealing and after prestrain

Aluminium alloy	Microyield and macroyield stresses (MPa)											
	1. Annealed for 2 h at 325° C		2. Immediate retest after (1)		3. Annealed for 65 h at 500° C after (2)		4. Immediate retest after (3)		5. After 106 days at 20° C after (4)		6. Immediate retest after (5)	
	Microyield stress	Macroyield stress σ_{ys}	Microyield stress	Macroyield stress σ_{ys}	Microyield stress	Macroyield stress σ_{ys}	Microyield stress	Macroyield stress σ_{ys}	Microyield stress	Macroyield stress σ_{ys}	Microyield stress	Macroyield stress σ_{ys}
Binary												
Al–5% Cr	20	345	250	400								
Al–12% Cr	14.6	300	170	350	8.2	55	101	125	75	135	125	172
Ternary												
Al–8% Cr–1.2% Fe	25	580	220	> 550	11.7	162	126	212	40	192	215	230

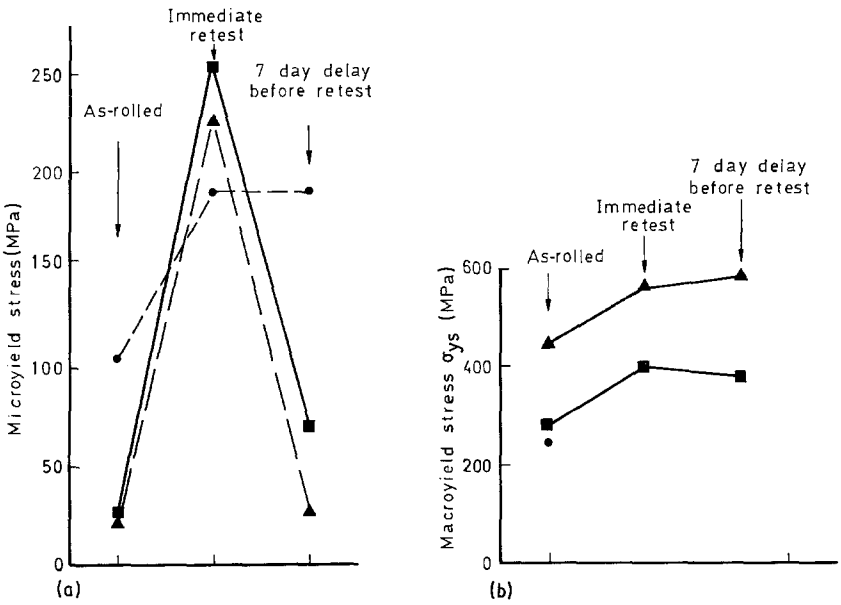

Figure 5 Microyield and macroyield stresses for as-rolled and prestrained vapour quenched alloys and commercial L70 Al-alloy. ▲, Al–6% Cr–1.0% Fe; ■, Al–5% Cr; ●, L70.

material in the previous test sequence (Curve 2, Table III). The σ_{ys} values were greater after prestrain and about equal to the maximum values before annealing (Table III).

Two alloys (Al–12% Cr and Al–8% Cr–1.2% Fe) were annealed further but at a temperature of 500° C for 65 h; this caused complete precipitation of the solute, a high volume fraction of particles and a small ($\leqslant 10\,\mu$m) recrystallized grain microstructure. There was no Stage 1 after this treatment, (Curves 3 in Figs 6b and c) and there was a large drop in the microyield and macroyield stresses (Table VI). Prestrain increased the microyield stresses, but they again decreased during rests at room temperature (Table VI). The stress level of the stress–strain curves of the vapour quenched Al–Cr alloy appeared to increase progressively with the number of load cycles (see Curves 3, 4, 5 and 6 lin Fig. 6b) but the curve for the Al–Cr–Fe alloy occurred at lower stresses after resting at room temperature (see Curves 4 and 5 in Fig. 6c).

The greater relaxation of the microyield stress in the ternary alloy compared with the binary alloy is apparent in Fig. 7a. The dependence on prestrain and on time was greater for the microyield stress than for σ_{ys} (Fig. 7b).

3.3. Tensile properties

The Al–12% Cr and Al–8% Cr–1.2% Fe alloy microstrain test pieces were pulled to fracture after retest (Curve 6 in Table VI). The tensile properties of the vapour quenched alloys in the as-rolled state and after the microstrain tests are given in Table V together with the tensile properties of the commercial aluminium alloys. Annealing the vapour quenched alloys at 500° C for 65 h caused large decreases in tensile strength and total elongation but had little effect on the uniform elongation and Young's modulus. Note the high Young's modulus values, up to 100 GPa in Al–12% Cr, are typical of vapour quenched alloys with these compositions [2].

The tensile strengths of the binary and ternary vapour quenched alloys in the as-rolled state varied from 0.9 to 1.5 times the tensile strength of the L70 alloy. Young's moduli for the vapour quenched alloys were between 1.2 and 1.4 times greater than the value for L70 alloy. However, the microyield stresses for vapour quenched alloys in the as-rolled state, or after annealing at 325° C and resting at room temperature, were only about 0.4 to 0.7 times the microyield stress of the L70 alloy.

4. Discussion

Because of the low microyield stresses and the extensive microstrain in vapour quenched alloys at stresses less than 100 MPa, these alloys are not suitable for use in gyroscopes. The microyield stresses obtained were comparable to those measured for commercial purity aluminium and much lower than the values for commercial aluminium alloys. This was in spite of the fact that the vapour quenched alloys had much higher tensile strengths and Young's moduli than the commercial alloys. Thus there was no correlation between the conventional tensile properties and the microyield stress. The difference between the mobile dislocation density in the vapour quenched alloys and in the commercial alloys is the most likely cause of the differences in microstrain behaviour. It is possible that unworked vapour quenched alloys with a much lower dislocation density would exhibit higher microyield stresses.

Once the dislocations have been introduced into the vapour quenched alloys, they are stabilized by the high solute concentration and by the high volume fraction of dispersed phase.

The commercial alloys either have a very low density of dislocations (e.g. alloys 2014–T6, 2024–T4, 6061–T6, Table III) or the dislocations are pinned by solute atoms and coherent precipitates (e.g. in alloys L70 and 5456–H34, Table III).

A three-stage stress–strain curve has been reported for other alloys in the microstrain region [4, 7, 8]. In nickel alloys after prestrain the stress–strain curves were similar in shape to Curve 1 in Fig. 3. The shape of the curves was explained in terms of the exhaustion of mobile dislocations at the end of Stage 1. A similar explanation may account for the shape of the stress–

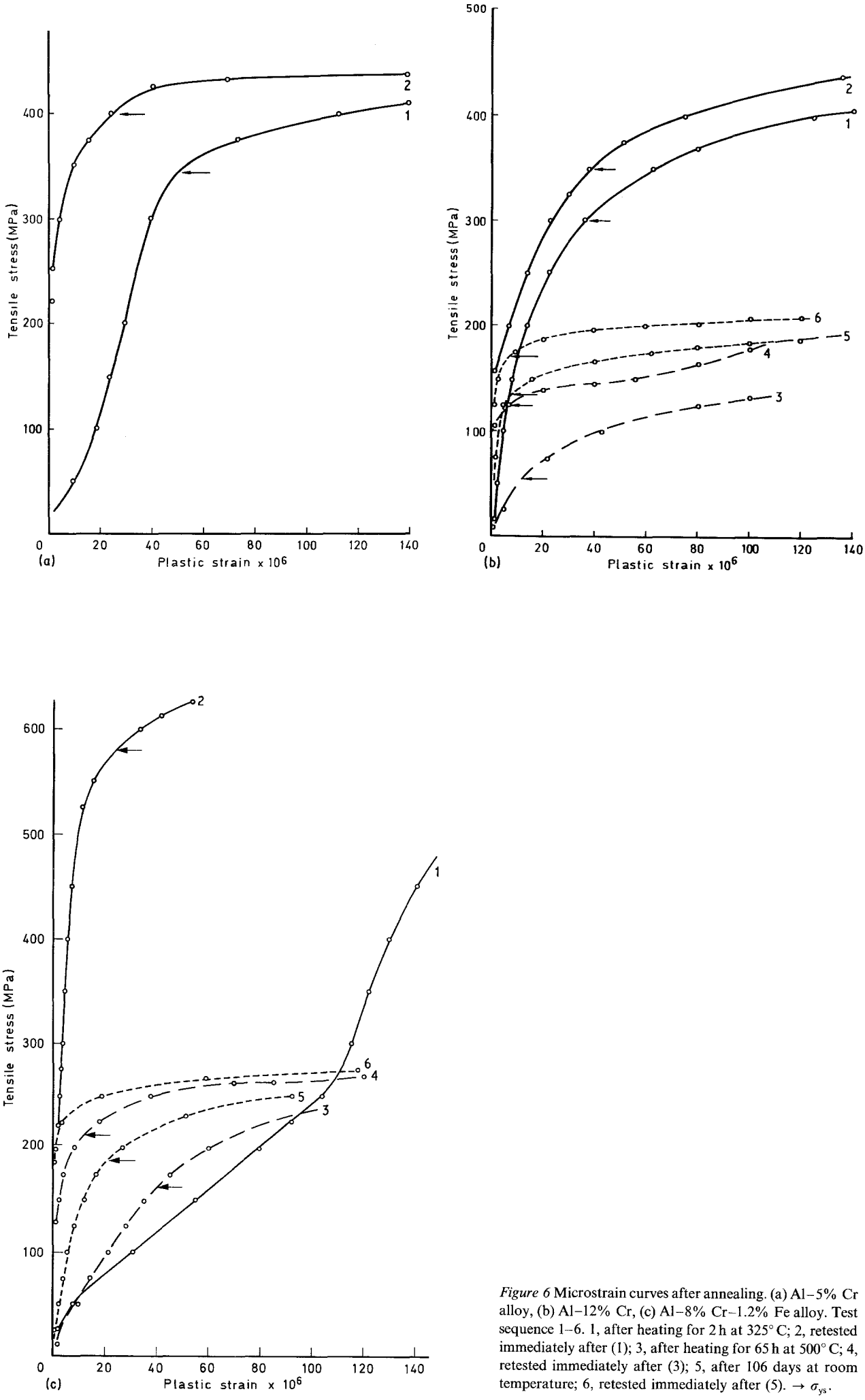

Figure 6 Microstrain curves after annealing. (a) Al–5% Cr alloy, (b) Al–12% Cr, (c) Al–8% Cr–1.2% Fe alloy. Test sequence 1–6. 1, after heating for 2 h at 325° C; 2, retested immediately after (1); 3, after heating for 65 h at 500° C; 4, retested immediately after (3); 5, after 106 days at room temperature; 6, retested immediately after (5). → σ_{ys}.

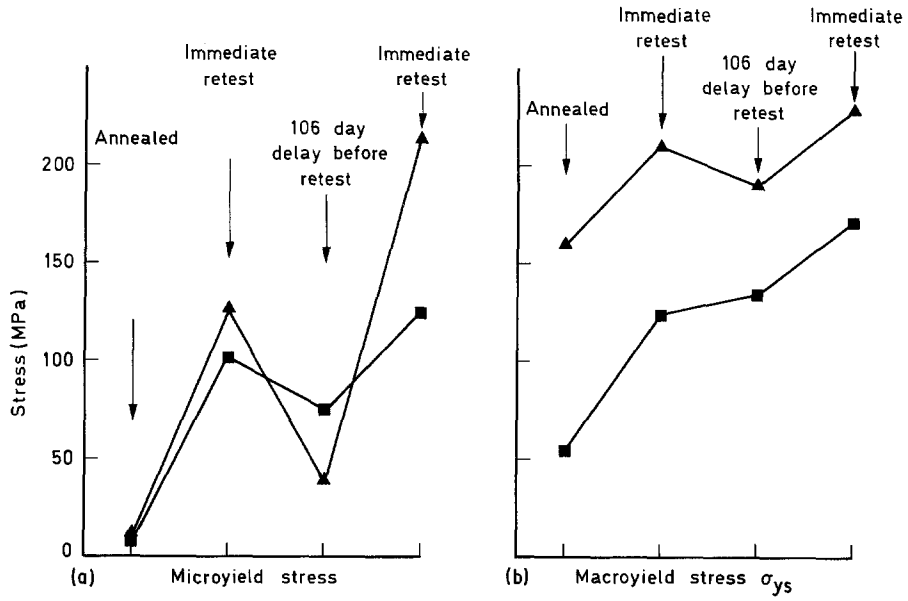

Figure 7 Microyield and macroyield stresses for vapour quenched alloys after 65 h at 500° C. ▲, Al–8% Cr–1.2% Fe; ■, Al–12% Cr.

strain curves in the vapour quenched alloys. Thus the strain ε is given by

$$\varepsilon = \varrho \boldsymbol{b} l \tag{1}$$

where ϱ is the density of mobile dislocations, $\boldsymbol{b}$ is the Burgers vector and l is the displacement of dislocation line.

If the displacement l is taken to be the separation between the particles of dispersed phase (20 nm) and ε is the strain measured in Stage 1 for the Al–6% Cr–1.0% Fe alloy (Fig. 3d) i.e. about 40×10^{-6}, then taking $\boldsymbol{b} = 2.84 \times 10^{-10}$ m, a value of $\varrho = 10^{13}\,\mathrm{m}^{-2}$ is obtained. Typically the dislocation density varies from $10^{10}\,\mathrm{m}^{-2}$ in annealed crystals to about $10^{16}\,\mathrm{m}^{-2}$ in heavily worked metals [9], so that a value of $10^{13}\,\mathrm{m}^{-2}$ may not be unreasonable for the vapour quenched alloys. A very high density of dislocations bowing between particles could explain the apparent low strain hardening in Stage 1.

The stress to produce a given strain increment will increase as the longer dislocation segments become pinned and the shorter dislocation segments become mobile. This could occur at the end of Stage 1 of the stress–strain curve and the strain hardening rate would then increase. This was observed in the vapour quenched alloys with exceptionally high strain hardening rates in Stage 2. For example for Curve 3 in Fig. 3d, a strain increment of 8×10^{-6} required a stress increment of about 400 MPa.

An estimate of the stress σ_{ys} required to cause flow at the end of Stage 2 can be obtained from the expression

$$\sigma_{ys} = \alpha \frac{G\boldsymbol{b}}{\lambda} \tag{2}$$

where $\alpha = 1$ for age-hardened aluminium alloys, λ is the distance between pinning points and G is the shear modulus. For $\lambda = 20$ nm and $G = 33$ GPa, a value of $\sigma_{ys} = 473$ MPa is obtained which agrees with the σ_{ys} values for as-rolled and prestrained material (Table III).

In the as-rolled state, Stage 1 was more evident in the ternary alloys (Curve 1 in Fig. 3c and d) than in the Al–5% Cr binary alloy (Curve 1 in Fig. 3a) and was absent in the Al–12% Cr binary alloy (Curve 1 in Fig. 3b). Although the strain hardening in Stage 2 ($\Delta\sigma$ in Fig. 4) was large in the binary alloys, the strain hardening rate was less than in the ternary alloys (Table IV). The differences in the microstrain curves reflected the different dislocation densities and mobilities caused by working temperature (higher in 5% Cr, Table I), working reduction (low in Al–12% Cr, Table I) and precipitate volume fraction and size. These differences between the binary and ternary alloys could be caused by a smaller volume fraction of dispersed phase in the binary alloys compared with the ternary alloys.

Large residual elastic stresses are present in vapour quenched aluminium alloy sheet in the as-rolled condition. In the Al–6% Cr–1.0% Fe alloy at 500 MPa after prestrain (Curves 2 and 3 in Fig. 3d) the elastic strains were between 280 and 470 times greater than the plastic strains. In a previous test [10] on a prestrained Al–Cr–Fe alloy test piece, completely elastic behaviour was found at a stress of ~ 600 MPa. The reduction in the microyield stress and the recurrence of Stage 1 in the vapour quenched alloys after resting at room temperature is attributed to the relaxation of these high residual stresses by dislocation glide. The relaxation effects observed after annealing at 650° C (Fig. 7) must be an indirect effect of the small grain size and large volume fraction of the precipitate.

The deformation of vapour quenched alloys under other conditions may be explained by the present results. For example the high strain hardening capacity could be responsible for the high fatigue limit in these alloys [11, 12]. In a notched fatigue test under a mean stress of P and a cyclic stress of $P \pm 0.9P$ and $K_t = 2.6$, the peak stress at the fatigue limit was 172 MPa, which corresponded to 447 MPa at the root of the notch. The yield stress σ_{ys} after prestrain was between 400 and 590 MPa. Thus the fatigue limit could be a consequence of cyclic strain hardening

in which the elastic strain becomes a progressively increasing fraction of the total cyclic strain. Similarly, enhanced strain during creep [10] and large Bauschinger hysteresis effects [10] may be associated with the high dislocation densities present.

Since it was impossible to decrease the dislocation density in vapour quenched and worked alloys by annealing without degrading the microstructure, a high dislocation density may be a characteristic feature of all high strength alloys produced by rapid solidification processing (RSP) and low temperature rolling. Microstrain data may therefore be needed in order to understand the deformation behaviour of these materials.

5. Conclusions

Vapour quenched and rolled Al–Cr and Al–Cr–Fe alloys had high tensile strengths and Young's moduli but low (< 26 MPa) microyield stresses compared with lower strength conventional Al-alloys. This was attributed to the presence of a high density of stable dislocations. The behaviour of these alloys may be typical of alloys produced by rapid solidification processing and rolling.

Acknowledgements

The authors are grateful to Mr R. L. Bickerdike for many helpful discussions during this research. This paper is published by the kind permission of the Royal Aircraft Establishment, Farnborough, Hants, UK.

References

1. R. L. BICKERDIKE, D. CLARK, J. N. EASTABROOK, G. HUGHES, W. N. MAIR, P. G. PARTRIDGE and H. C. RANSON, *Int. J. Rapid Solidification* **1** (1985) 305.
2. *Idem, ibid.* **2** (1986) in press.
3. R. D. CARNAHAN, *J. Metals* (1964) 990.
4. W. BONFIELD, in Proceedings of the AGARD Conference on Inertial Navigation Components and Systems. No 116 (1973) p. 6-1.
5. C. W. MARSCHALL and R. E. MARINGER, *J. Materials* **6** (1971) 374.
6. W. BONFIELD and C. H. LI, *Acta Met.* **11** (1963) 585.
7. W. BONFIELD and P. K. DATTA, Final report ER 4050, PARTS I–II July (1973).
8. R. D. CARNAHAN and J. E. WHITE, *Phil. Mag.* **10** (1964) 513.
9. F. A. McCLINTOCK and A. S. ARGON, "Mechanical Behaviour of Materials" (Addison-Wesley, Reading, Massachusetts, 1966) p. 106.
10. P. G. PARTRIDGE, unpublished work (1980).
11. J. WEERTMAN and J. R. WEERTMAN, "Physical Metallurgy" (North Holland, 1965) p. 789.
12. W. BONFIELD, *Scripta Met.* **6** (1972) 77.

Received 3 October
and accepted 7 November 1985